

Electrical conduction of chalcogenide $\text{Se}_{90}\text{Te}_{10-x}\text{Ag}_x$ ($x=0,2,4\&6$) films

A .S. Farid¹, N. A. Hegab¹

Physics Department, Faculty of Education , Ain Shams University, Cairo, Egypt

Abstract

Four different $\text{Se}_{90}\text{Te}_{10-x}\text{Ag}_x$ ($x=0,2,4\&6$) compositions were prepared by melt quenching technique. Thin film samples(165-711nm)were obtained from the studied compositions by thermal evaporation technique. The current –voltage(I-V) characteristics have been measured throughout the temperature range (298-323 K). The obtained I-V curves are composed of two regions, low field region(ohmic conduction) and high field region (non-ohmic conduction). The analysis of the ohmic current reveals that the conduction takes place through a thermally activated process, and the activation energy values are evaluated for the film compositions. The high field region of the I-V curves have been analyzed on the basis of modified Poole-Frenkel mechanism. The effect of Silver addition was investigated. The variation of dielectric constant with temperature was investigated for the studied film compositions.

Key words: Chalcogenide glasses. Conduction mechanism. Activation energy

1.Introduction

The study of direct conduction in electric current through amorphous thin films is increasing in recently years to explore the electrical

conduction properties. Among these materials chalcogenide semiconductors are new kind of materials with great qualities of use in fabrication of microminiaturized electronic components which is useful in microelectronic industry such as , computer memories, erasable density optical memories, photoconductive applications such as photoreceptors in copying machines and X-ray imaging plates ,IR optical lenses and windows and high sensitivity ionic sensors[1-4]. This class of materials belong to the group of non oxide glasses.

In recent years, enormous interest has been devoted to study the physical properties, structure, photoeletronic, thermal and optical properties of Se-Te chalcogenide alloys[5-8]. This is because theses alloys are characterized by the great hardness, high photo sensitivity and high crystallization temperature[9]. It is recognized that the addition of third element to a Se-Te system causes structural changes in the material and leads to modify the band structure and hence the electrical properties. It is known that Silver diffuse very easily in chalcognide glassy matrix, bridging the chalcognide chains and hence leads to more stable structure. All reported studies varying the percentage of Ag addition at the expense of Se, but there few works are reported in literature with the Ag addition at the expense of Te. From this point of view, this paper repots the study of some electrical properties of Se-Te with Ag addition and investigate the conduction mechanism in the $Se_{90}Te_{10-x}Ag_x$ ($x=0,2,4\&6$)films as a function of both applied voltage and temperature through the temperature range(298-323K) and thickness range(165=711nm).

2. Experimental details

Four different $Se_{90}Te_{10-x}Ag_x$ ($x=0,2,4\&6$) bulk compositions were prepared by melt quenching technique[10]. The proparate amount of the constituent elements of Se,Te and Ag of high purity 99.999% are sealed in evacuated silca tubes (0.2m length , 0.01mdiameter) of 10^{-5} Torr.

Synthesis was carried out in an oscillatory furnace(3 turn/min)to ensure the homogeneity of the composition. The temperature of the furnace was raised in steps with rate(4K/min) to 1300 K and kept at this temperature for 10h. Then each tube was quenched in icy water to obtain the synthesized material in the amorphous state. Thin film samples of sandwich configuration with different thicknesses were prepared by thermal evaporation technique on dry clean glass substrates using coating unit (Edwards type E306A). The substrate temperature was held at that of the room during the deposition process. The film thickness was determined after evaporation by Tolansky's interferometric method[11]. The chemical composition of the film samples is checked by energy dispersive analysis(EDX) using scanning electronic microscope(Joel 5400)[10]. X-ray diffraction showed that the obtained films samples possessed amorphous structures as illustrated in Fig.(1) .

I-V characteristics were measured in the temperature range 298-323 K below the glass transition temperature for the studied compositions, using an electrometer (Keithley type 616A) for potential drop measurements and a microdigital multimeter (HC-5010-EC) for the current measurements. The temperature of the sample was measured by using a chromel – alumel thermocouple attached to the sample.

3. Results and Discussion

3.1. I–V characteristics

The current-voltage (I–V) characteristics were measured for $\text{Se}_{90}\text{Te}_{10-x}\text{Ag}_x$ at different elevated temperatures (298 to 323 K) and different thicknesses(165-711nm).Fig.2(a-d) represents the I-V characteristic curves for one thickness of each composition at different elevated temperatures. This figure declares that the I-V curve is linear at lower voltage(ohmic behavior) and become non-linear at higher voltages.

There are several mechanisms can be used to interpret these curves such as space-charge limited conductivity and the Pool-Frenkel(PF) or Schottky(Sc)effects. The current-voltage(I-V) characteristics plotted on a Log-Log scale didn't pointed to any conduction mechanism. Thus the data of Fig.2(a-d) must be re-plotted as Log I vs $E^{1/2}$ scale. Fig.3(a-d)shows the plots of(Log I vs $E^{1/2}$) for the studied film compositions. . The field dependence of the current referred that the conduction mechanism may be either the Schottky [12], or Poole-Frenkel [13] type. In order to differentiate between the two types of conduction mechanisms, the following rules will be examined: a) $\text{Log}IT^{-2}$ should vary linear with T^{-1} at different fixed applied voltage. This is not verified in any compositions of the studied system. (b) The Scottcky mechanism demands that the activation energy should be greater than 0.8eV, while the obtained values lie in range 0.53-0.77eV. (c) By extrapolating the obtained curves in Fig.3(a-d) ($\text{Log}I-E^{1/2}$) to zero applied field, they don't pass through this point. These results ensure that the Schottky emission don't the operative mechanism and the field dependence was the property of the bulk material.

Considering the Poole-Frenkel effect, where the electrons are thermally emitted from the donor centers or randomly distributed traps to the conduction band by the lowering of the Coulombic potential barrier when it interacts with an external field, the current density (J) in thin film containing shallow traps and hence a field dependence is expressed by the following relation[14]:

$$J = J_0 \exp(\beta E^{1/2}/kT), \quad (1)$$

Where J_0 is the low field current density, E is the applied electric field, k is the Boltzmann constant, T is the absolute temperature and β is the field lowering coefficient which is given by:

$$\beta = (e^3/n\pi\epsilon\epsilon_0)^{1/2}, \quad (2)$$

where $n=1$ for Poole-Frenkel emission and $n=4$ Schottky emission, e is the electronic charge, ϵ_0 is the permittivity of the free space ($\epsilon_0=8.82 \times 10^{-12}$, Fm^{-1}), and ϵ is the dielectric constant of material. Since, β is an essential factor that determines the magnitude of the columbic field [15]. Thus the values of β_{PF} and β_{Sc} are calculated by using the values of ϵ given in Table.(1) for the studied compositions obtained from our dielectric study. The experimental values of β_{PF} obtained from the slope of Fig.3(a-d) are given in Tables.(2) for the studied film compositions. It is observed from Tables.(2) that β_{PF} increases with increasing temperature, moreover the experimental value of β_{PF} is approximately (1.46-2.079) times the theoretical value for $\text{Se}_{90}\text{Te}_{10}$ films as representative example and $\beta_{\text{Sc}}=1/2 \beta_{\text{PF}}$. Thus we conclude that the predominant conduction mechanism in the studied films is Poole-Frenkel type, which is better than Schottky effect. On the other hand the agreement between the theoretical and experimental values of β_{PF} can't be taken as an indicating factor for specifying the responsible conduction mechanism.

Several investigators have observed a field dependent conduction as expressed by Equ.(1) in what is apparently bulk limited conduction . There are various models are put forward to explain the anomaly of the obtained values of β . The first explanation [16] pointed to the presence of neutral traps and a deep donor level at energies E_t and E_d with the Fermi level located centrally between them. E_t and E_d were measured from the bottom of the conduction band.

According to Hill[15] who assumed that donors and traps co-exist and that the density of ionized donor is only a small fraction of the total density of ionizing donor. If this is the case then ionization of donor by Pool-Frenkel emission can stimulate further ionization by other process. The initial ionized donor acts as a capture centre for the electron released from the second donor, giving rise to an effective mobile donor and

anomalous value of β . In neutral centers each lying at energy E_i below the bottom of the extended states in the conduction band, after emission of an electron from the donor. It has been trapped within the coulombic well of the ionized donor, subsequent de-trapping and movement of this carrier in the well would result in the Pool-Frenkel effect. However during the time of trapping the carrier, it is possible for a second ionized event to occur. Once an electron neutralizes another donor, the potential barrier between the first and second donor decreases by the overlapping of two potential wells, and thermal emission of electrons can now occur over this lowered coulombic barrier by the external electric field, to the conduction band.

3.2. I-T characteristics

The variation of the current with temperature in the range (298-323K) was examined for the as deposited $\text{Se}_{90}\text{Te}_{10-x}\text{Ag}_x$ ($x=0$ and 6 at.%) films as example at constant applied voltage in the low field since the conduction in most semiconductors obeys ohm's law. This variation is controlled by the following relation:

$$I = I_0 \exp - \Delta E_\sigma / kT, \quad (3)$$

Where, ΔE_σ is the activation energy, I_0 is the current extrapolated to $1/T = 0$. Figs. 4(a-d) represent the relation between (I (in logarithmic scale) versus $1/T$) at different constant applied voltage for the studied films. It is clear from this figure that the obtained curves are straight lines, indicating that the conduction in these films is thermally activated type having single activation energy through the studied temperature range. Also the slopes of these curves for each composition of the studied system. Films seemed to be not vary apparently with the applied voltage. This can be explored from the obtained values of the activation energy for

each composition listed in Table.(3). This table declare that the activation energy value increases with the increase of Ag concentration in the studied compositions, i.e. the Te/Ag ratio decreases. Since Ag atoms make bonds with Se and Te atoms, resulting in more Se-Ag bonds with higher strength than the other bonds present in the network[17](see Table.(4)), and consequently a decrease in the conductivity. Similar results are obtained before[18]. It is concluded that the change of composition plays a pronounced effect in determine the density of donor or acceptor and traps. This change leads to an increase in the structural disorder and presence of localized states at deep acceptor and donor levels in the energy gap of the materials.

3.3. Poole-Frenkel mechanism and its modification

In order to decide whether the Poole-Frenkel effect is operating in the high field region an extrapolation was advanced in terms of modified Poole-Frenkel effect based on the thermal ionization of donor and hopping process. This demand to plot the data of Fig.2(a-d) in accordance to high electric field theory. Fig.5(a-d) illustrates a plot of $\text{Log } IE^{-1}$ vs $E^{1/2}$ (in logarithm scale). The obtained relations are linear as required by the Poole-Frenkel equation [19]. The obtained results of β_{PF} and ϵ are given in Table.(2). It is observed that β_{PF} values for $\text{Se}_{90}\text{Te}_4\text{Ag}_6$ films obtained from the slope of the studied straight lines is $2.985 \times 10^{-5} \text{, eV m}^{-1/2}$ is lower than that derived theoretically while, the values of the dielectric constant is much higher than that given in Table.(1). The values of β_{PF} generally show an increase with increasing temperature and decreasing with increasing Ag content.

Let us now analyze the results in the light of Jonscher's model[20]which takes account of the emission of electrons from sites in

one particular direction in space(all other directions having a higher energy barrier to electron motion).with respect to the applied electric field. Fig.6(a-d) illustrates $\text{Log } IE^{1/2}$ vs $E^{1/2}$ characteristics which are linear and the derived values of β_{PF} and ϵ are given in Table.(5) for the studied films. Fitting the obtained data with the Jonscher model result in an indication that a modified Poole-Frenkel is operating.

Fig.7(a-d) depicts the plots of $\text{Log } IE^{-1/2}$ vs $E^{1/2}$ for the conduction model based on the assumption that the charge carriers are travel for a constant period of time before being trapped. The obtained plots are linear, and Table.(5) illustrates the deduced values of β and ϵ for the studied film compositions. Theses tables declare that there is a large change in β and ϵ occurred with increasing temperature. Thus it is seen that the modified theory of Jonscher can explain this change. It is established for amorphous materials, the exponential increase in current at high fields may be due to an increase in the mobile carrier concentration, to field assisted thermal activation of electrons and holes initially localized at the deep donor and acceptor levels into the extended band states.

It is assumed that the dc high field conduction mechanism in amorphous films can be explained on the basis of the general conduction equation based on the ionization of the local defects by applied electric fields[15]. Also the amorphous films are characterized by the presence of localized levels in the forbidden energy gap due to their amorphous nature. These localized levels act as Pool Frenkel centers[21]. Theoretical study [21,22] on the electronic structure of disordered materials implies that the localized states exist near the band edges, rather than extending throughout the conduction bands. Besides the stated extend through the energy states near the band edges are also localized(traps) and are formed inside the forbidden gap.

4. Conclusions

The I – V characteristics of thermally evaporated $\text{Se}_{90}\text{Te}_{10-x}\text{Ag}_x$ ($x = 0, 2, 4, 6$ at. wt%) were obtained at temperature range (298-323K) and thickness range (165-711nm). Analysis of the I-V curves shows ohmic conduction at lower electric field values (linear shape) and become non linear at high electric field values (non ohmic). The analysis of the I-V characteristics revealed that $\log I$ versus $E^{1/2}$ obeys Poole-Frenkel mechanism. Further studies indicate that the conduction mechanism follows Jonscher modified dependence follows Poole-Frenkel mechanism. This is observed. The I-V characteristics in the non-ohmic region can be understood in terms of both simple and modified Poole-Frenkel mechanisms. The temperature dependence of the current in the ohmic region studied through measuring range shows a thermally activated process with a single activation energy ΔE_{σ} . It is found that the activation energy increases with increasing Ag content in the studied compositions due to the increase of the density of stronger bonds in the structure of the studied compositions.

References

- [1] A N Sreeram, A K Varshneya and D R Swiler *J.Non-Cryst.solids* **130** 225 (1991)
- [2] S R Ovshinsky, *Phy.Rev.Letters* **21** 1450 (1968)
- [3] A Felz *VCH Amorphous Inorganic Materials and Glasses*, Weinheim, Germany (1993)
- [4] V F Kokorina *Glasses for Infrared Optic*, CRC press, Boca Roton FL (1996)
- [5] S E Elliot *Material Science and Technology Chacogenide glasses*, New York (1991)
- [6] N Mehta, D Sharma, A Kumar *Physica B* **391** 108 (2007)
- [7] Satish Kumar, M Husain, M Zulfequar *Physica B* **371** 193 (2006)
- [8] N Mehta, A Kumar *Mter Chems and Phys* **96** 73 (2006)
- [9] B T Kolomiets *Phys.Stat. Sol(a)* **77** 13 (1964)
- [10] A E Bekheet, N A Hegab, M A Afifi, H E Atyia, E R Sharaf *Appl.Surf Science*, **252** 4590 (2009)
- [11] A Tolansky *Introduction to Interferometry*, Longman, New York (1951)
- [12] W Scottky *Z Physik* **15** 872 (1914)
- [13] J Frenkel *Phys. Rev.* **54** 647 (1938)
- [14] C A Mead *Phy.Rev* **128** 2088 (1962)
- [15] R M Hill *Phil. Mag.* **23** 59 (1972)
- [16] J G Simmons *Phys.Rev* **155** 595 (1967)
- [17] N F Mott *Adv.Phys.* **16** 49 (1967)
- [18] N F Mott *Phil.Mag.* **19** 835 (1969)

[19] L Pauling *the chemical bond cornell university press* (1960)

[20] N A Hegab *J.Phys.D.Applied phys.***33** 2356(2000)

[21] J Frenkel *Phys. Rev.* **54** 647(1938)

[22] A K Jonscher *thin solid films.***2**(1968)**185**, ibi 1(1967)

List of Figures

Fig.(1): X-ray diffraction patterns for $\text{Se}_{90}\text{Te}_{10-x}\text{Ag}_x$ ($x = 0, 2, 4$ and 6) films of nearly the same thickness.

Fig.2(a-d): I-V characteristics curves at various temperatures for $\text{Se}_{90}\text{Te}_{10-x}\text{Ag}_x$ ($x = 0, 2, 4$ and 6) films.

Fig.3(a-d): $\log I$ versus $E^{0.5}$ at different temperatures for $\text{Se}_{90}\text{Te}_{10-x}\text{Ag}_x$ ($x = 0, 2, 4$ and 6) films.

Fig.4(a-d): $\log I$ versus $1000/T$ at different applied voltage values for $\text{Se}_{90}\text{Te}_{10-x}\text{Ag}_x$ ($x = 0, 2, 4$ and 6) films.

Fig.5(a-d): $\log I E^{-1}$ versus $E^{0.5}$ at different temperatures for $\text{Se}_{90}\text{Te}_{10-x}\text{Ag}_x$ ($x = 0, 2, 4$ and 6) films.

Fig.6(a-d): $\log I E^{0.5}$ versus $E^{0.5}$ at different temperatures for $\text{Se}_{90}\text{Te}_{10-x}\text{Ag}_x$ ($x = 0, 2, 4$ and 6) films.

Fig.7(a-d): $\log I E^{-0.5}$ versus $E^{0.5}$ at different temperatures for $\text{Se}_{90}\text{Te}_{10-x}\text{Ag}_x$ ($x = 0, 2, 4$ and 6) films.

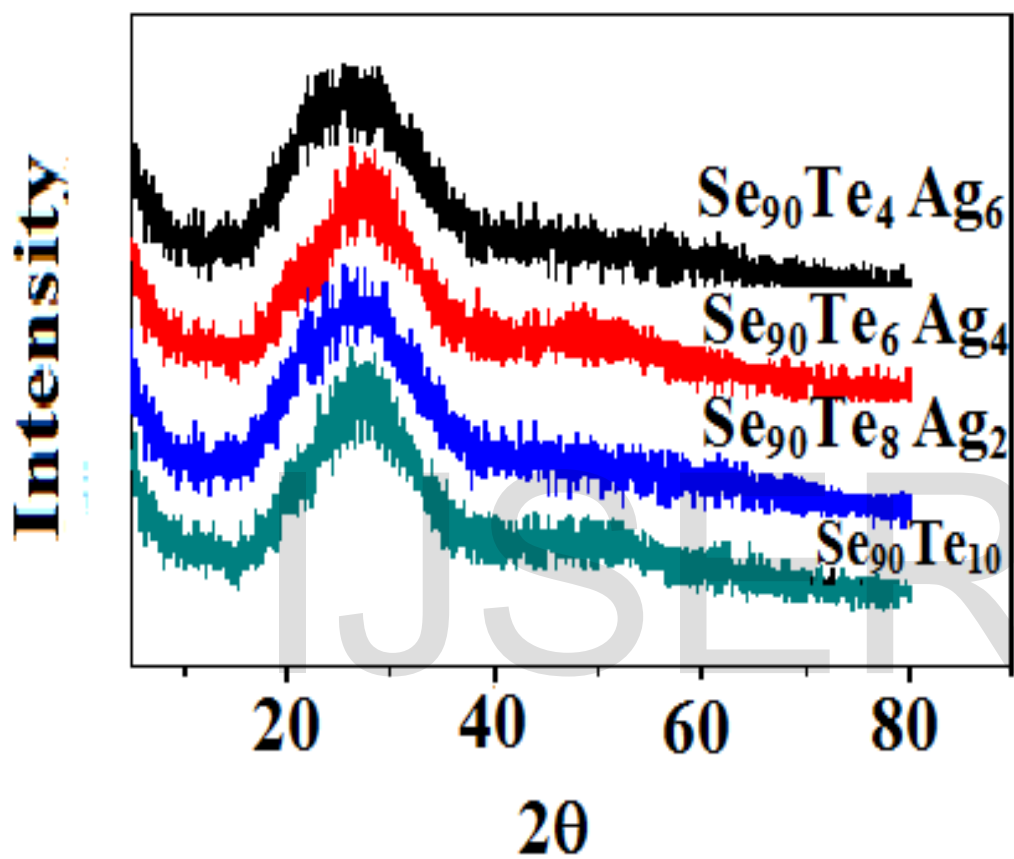


Fig.(1)

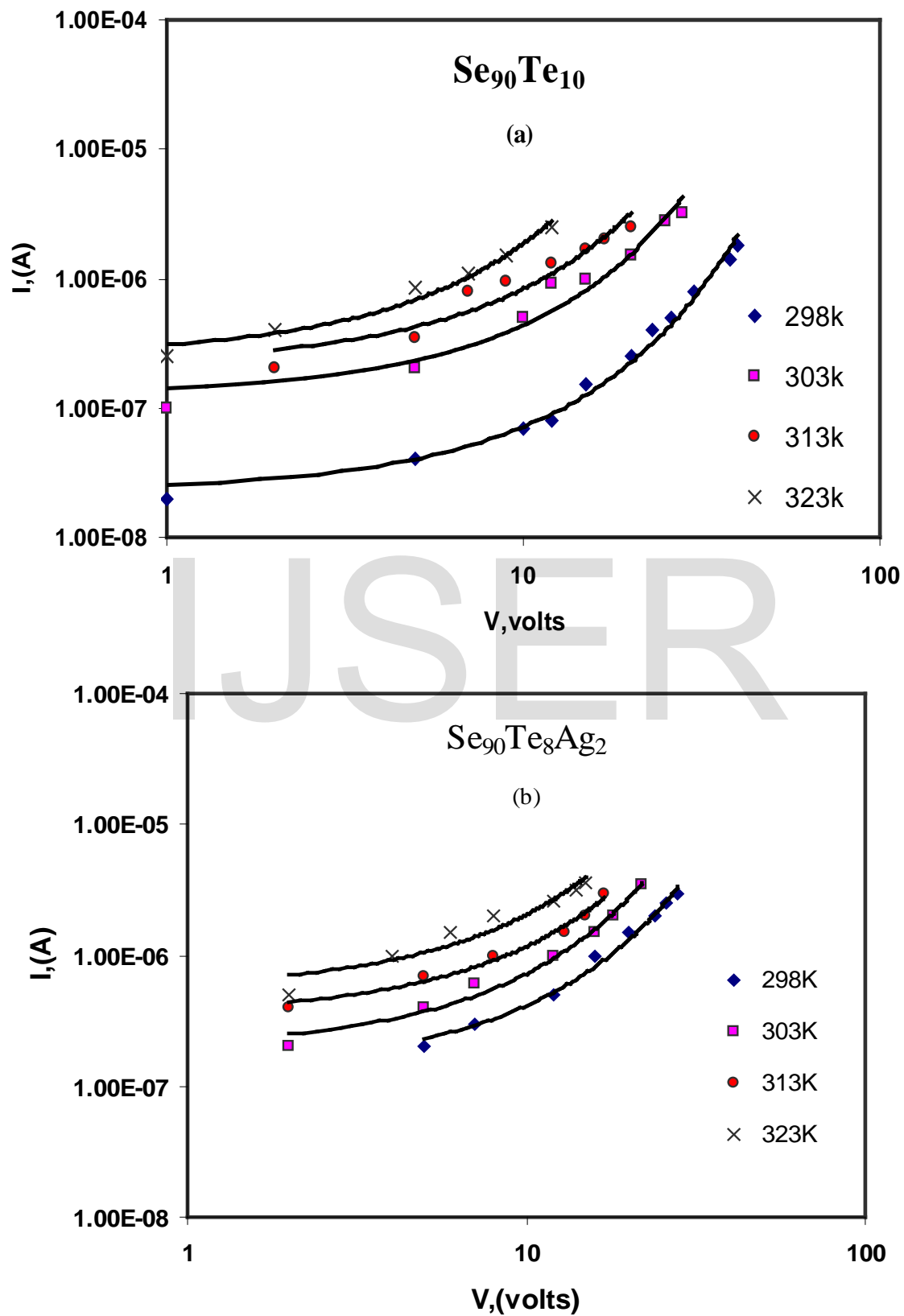


Fig.2(a,b)

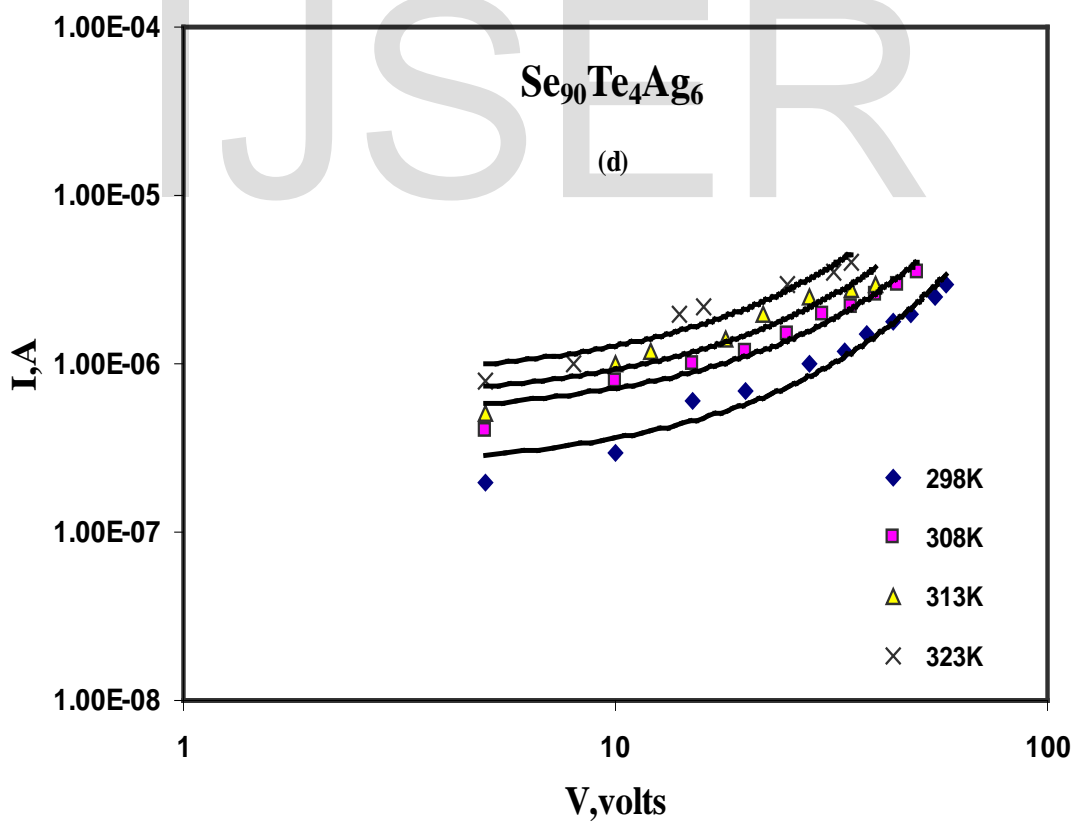
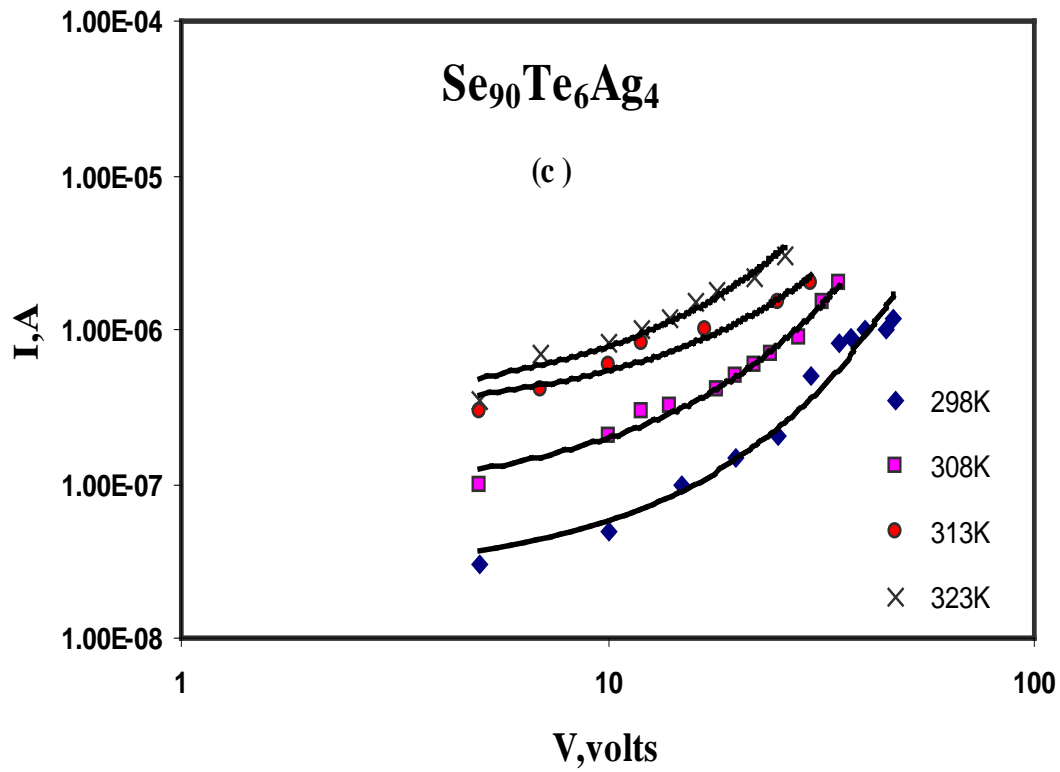


Fig.2(c,d)

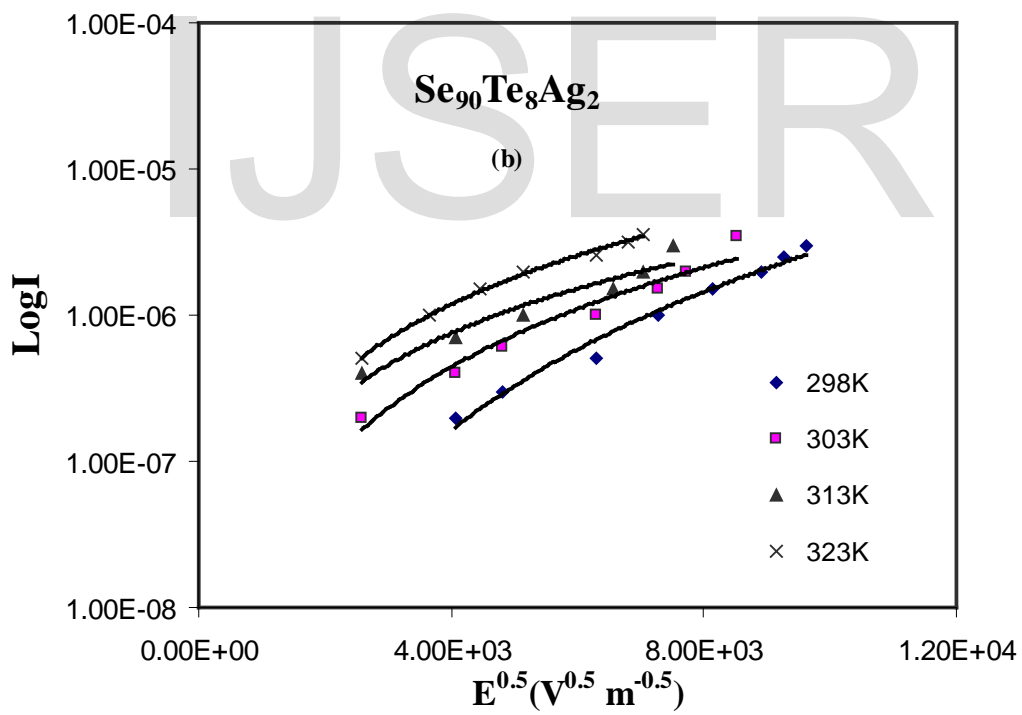
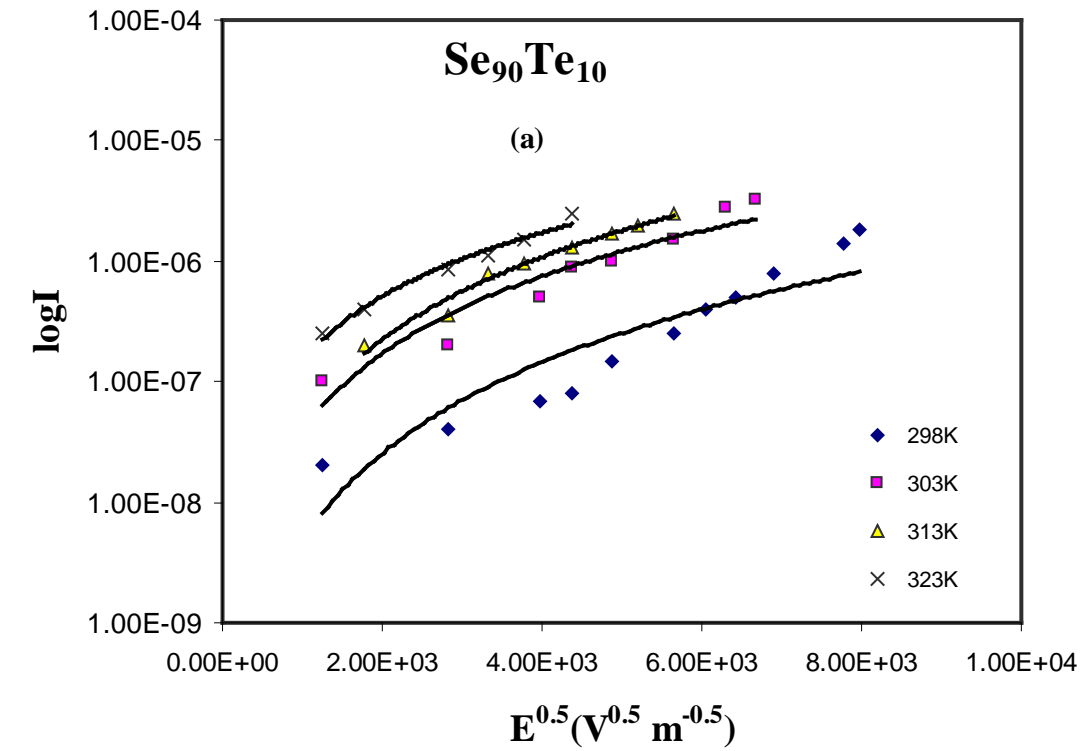


Fig.3(a,b)

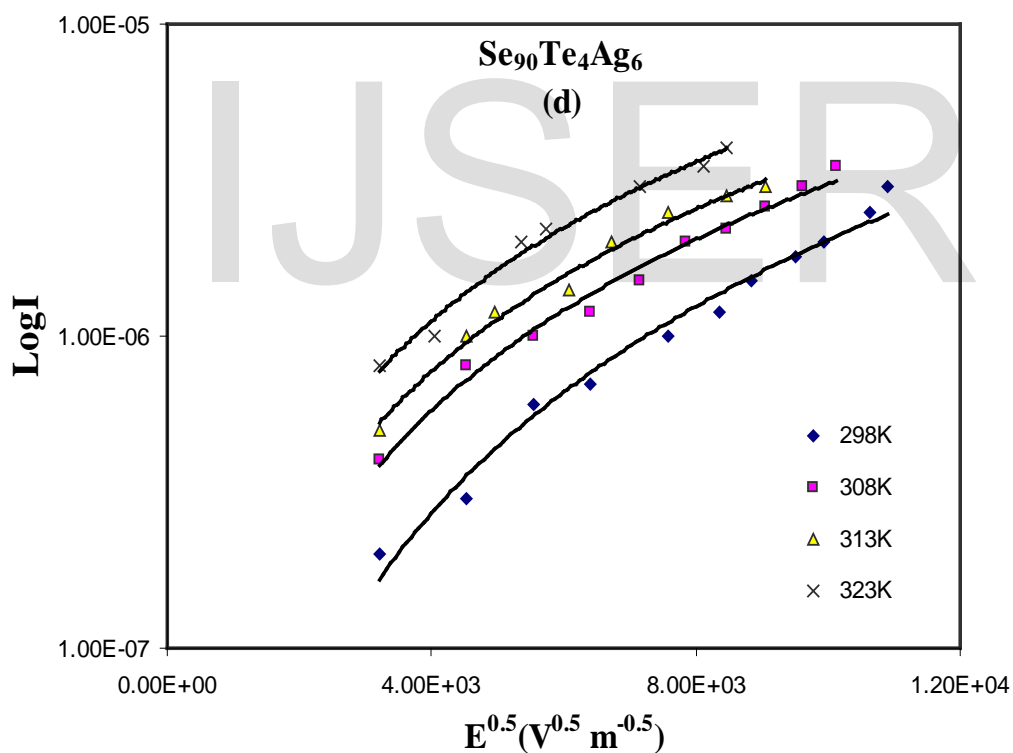
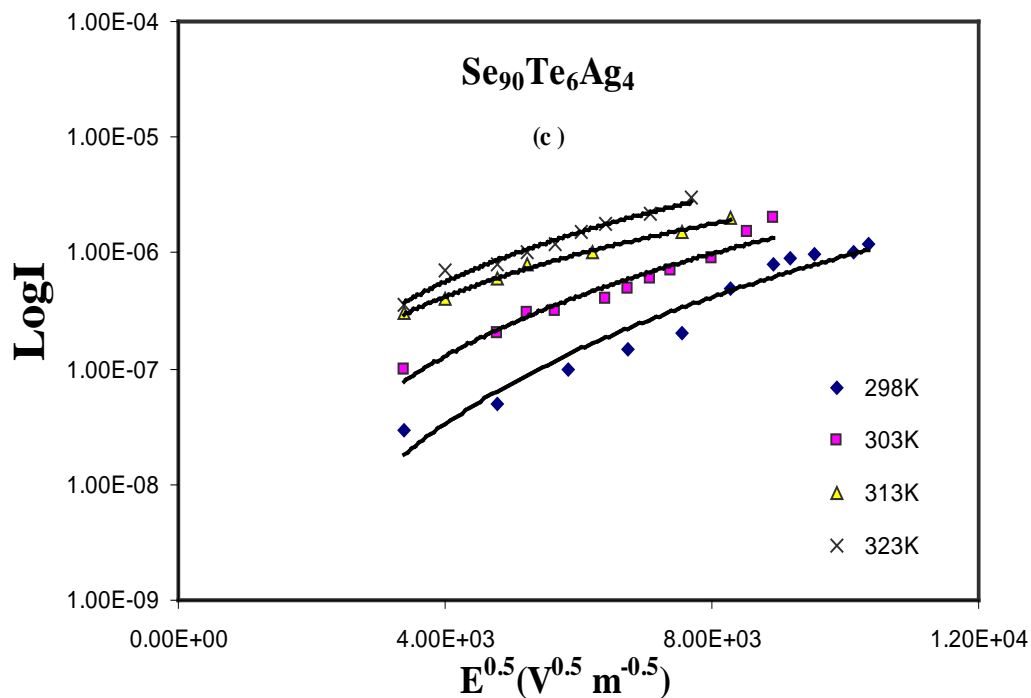


Fig.3(c,d)

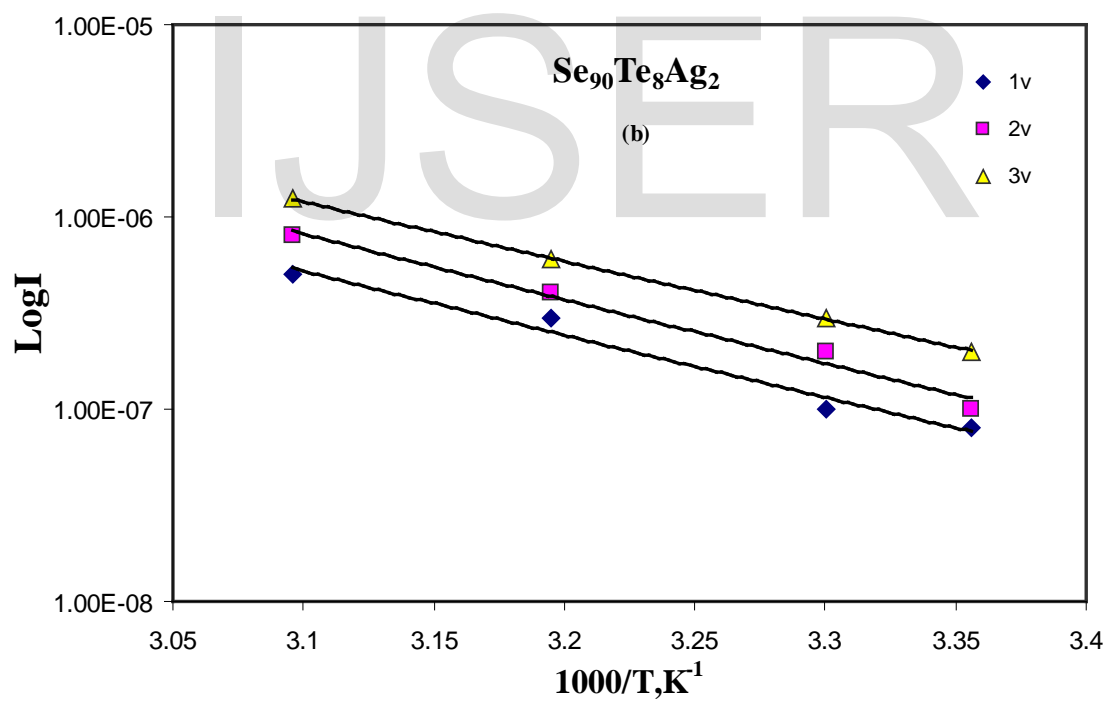
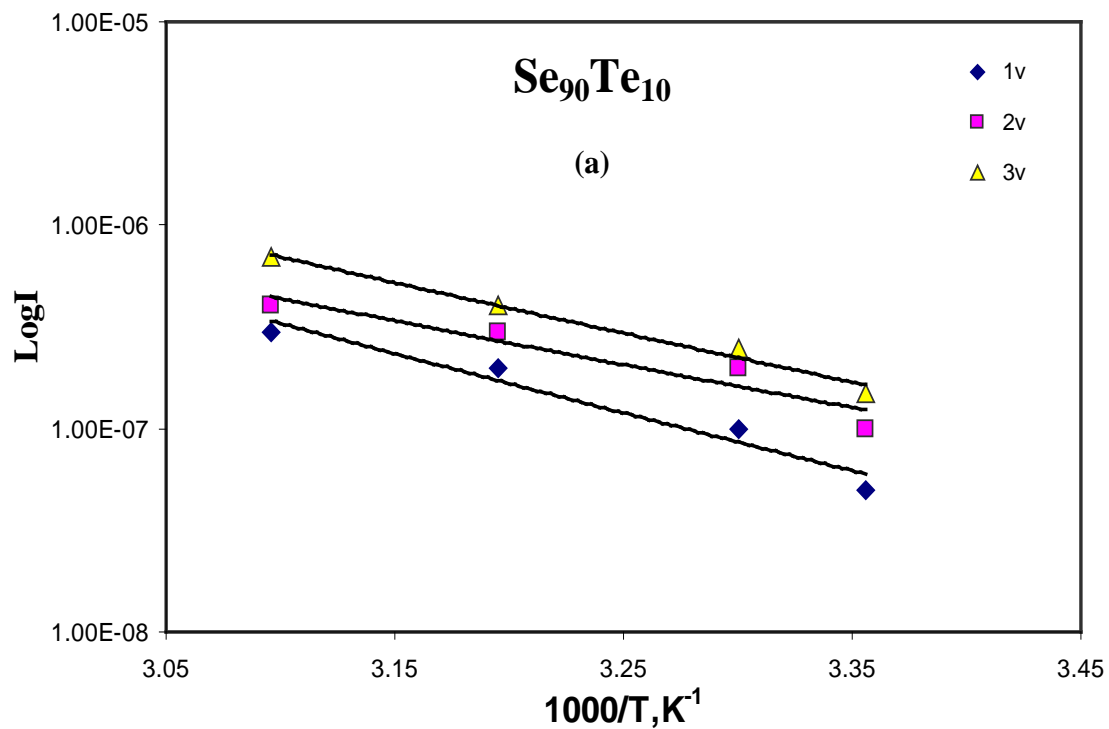


Fig.4(a,b)

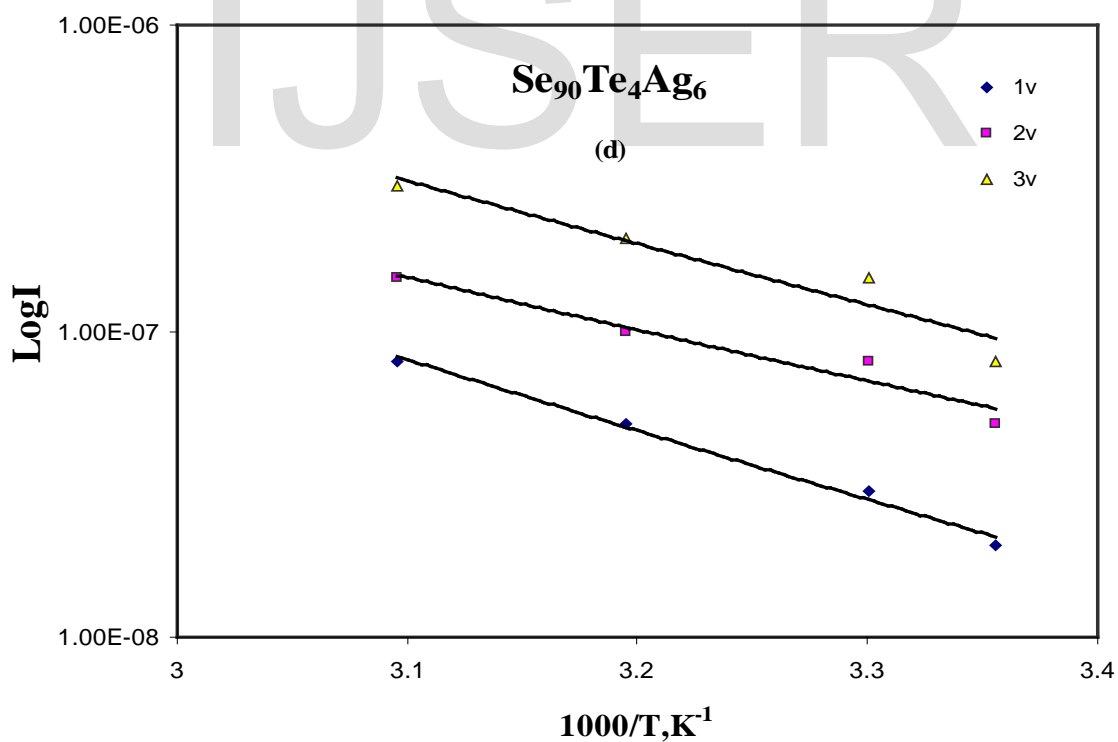
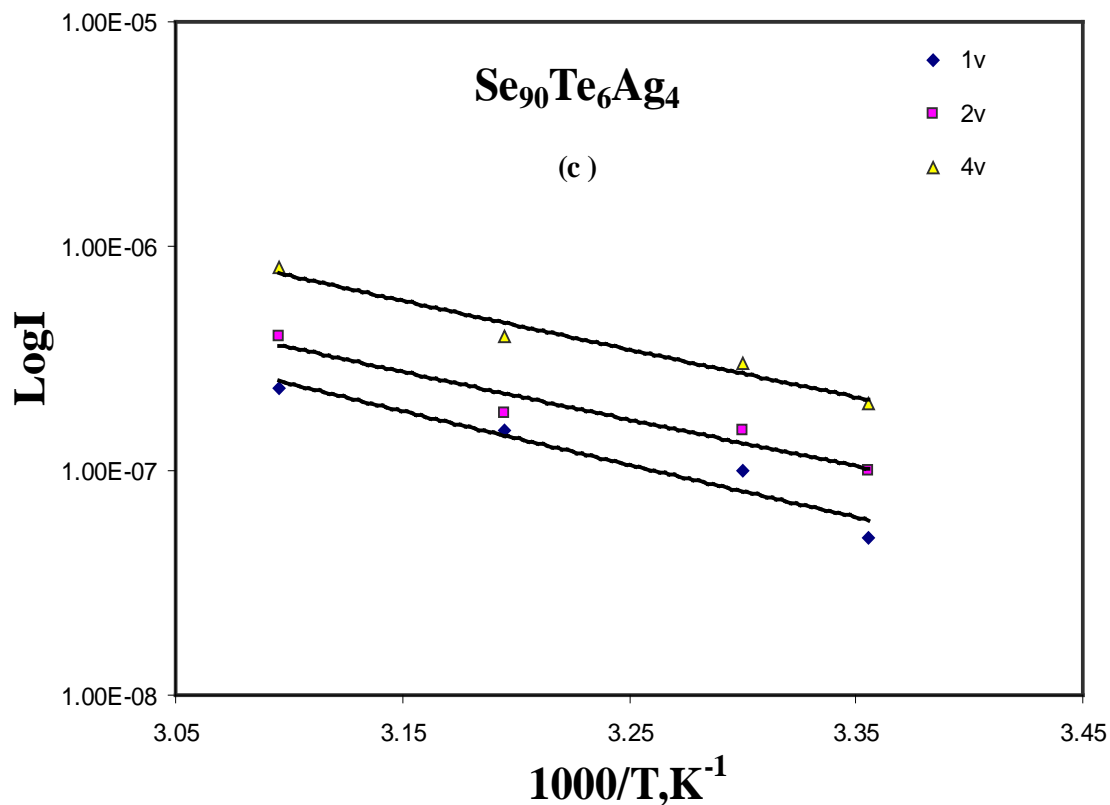


Fig.4(c,d)

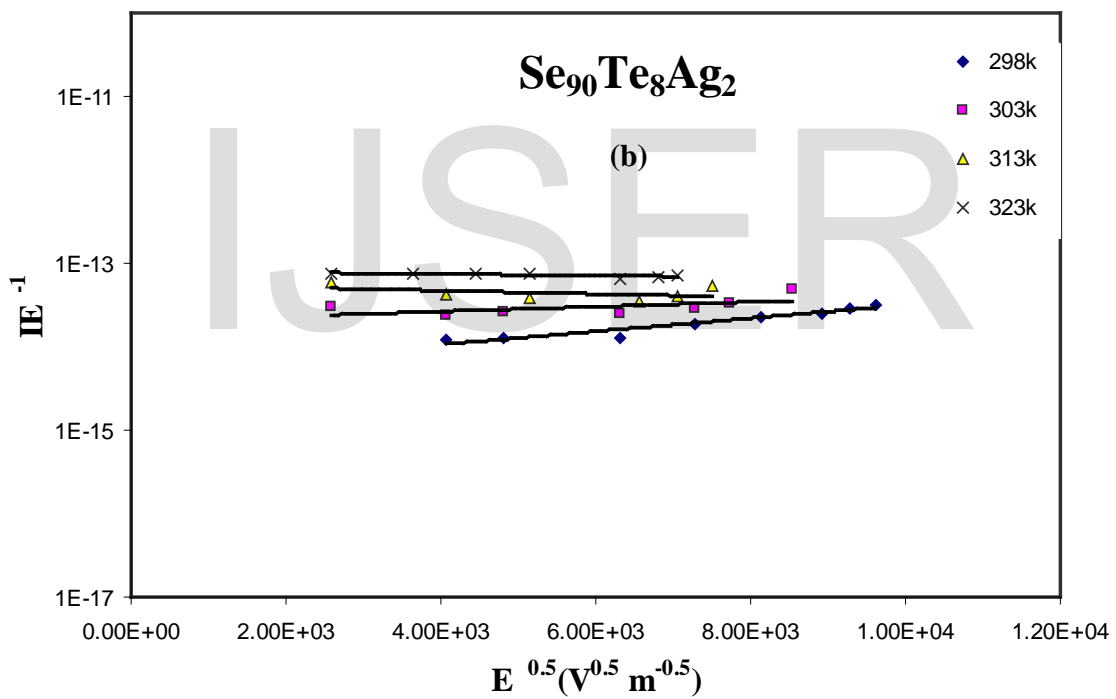
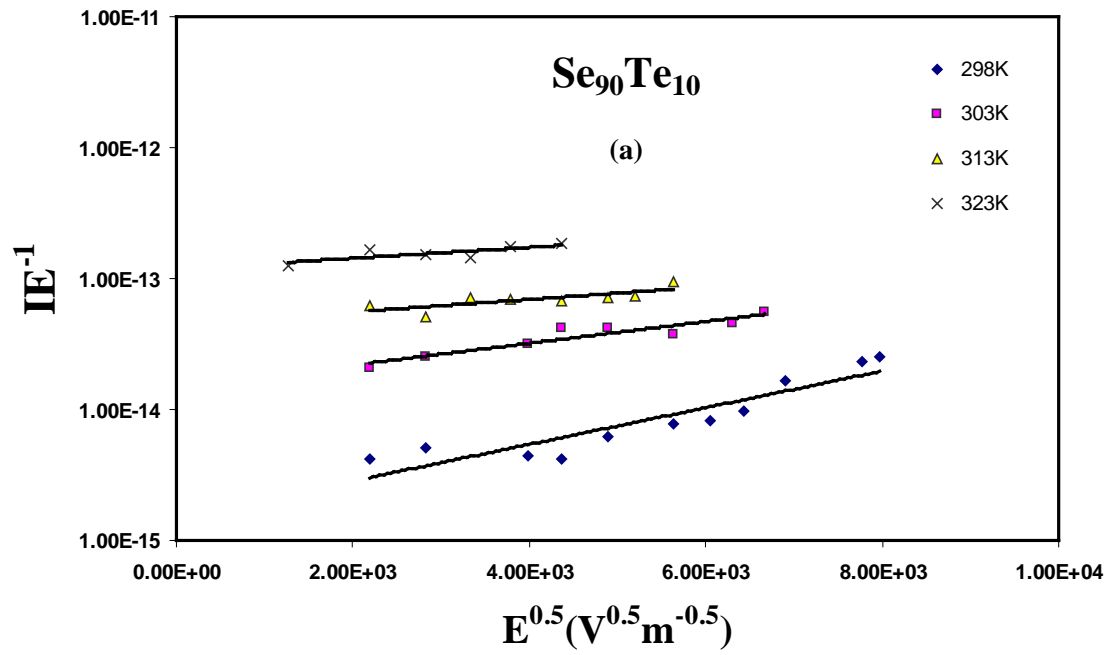


Fig.5(a,b)

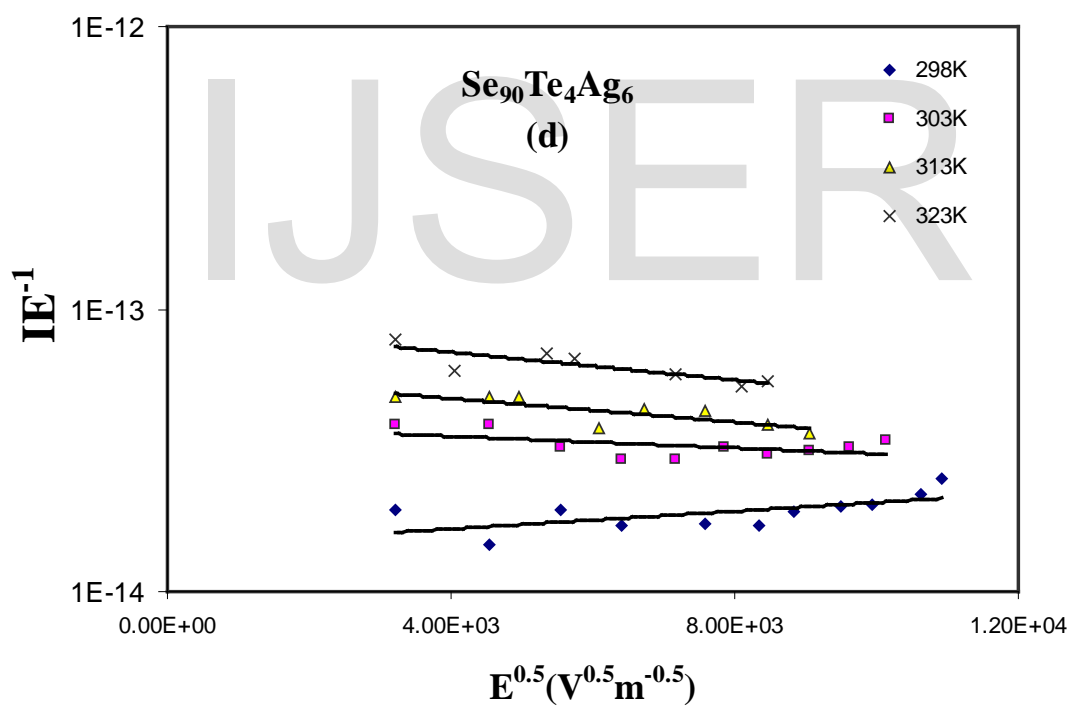
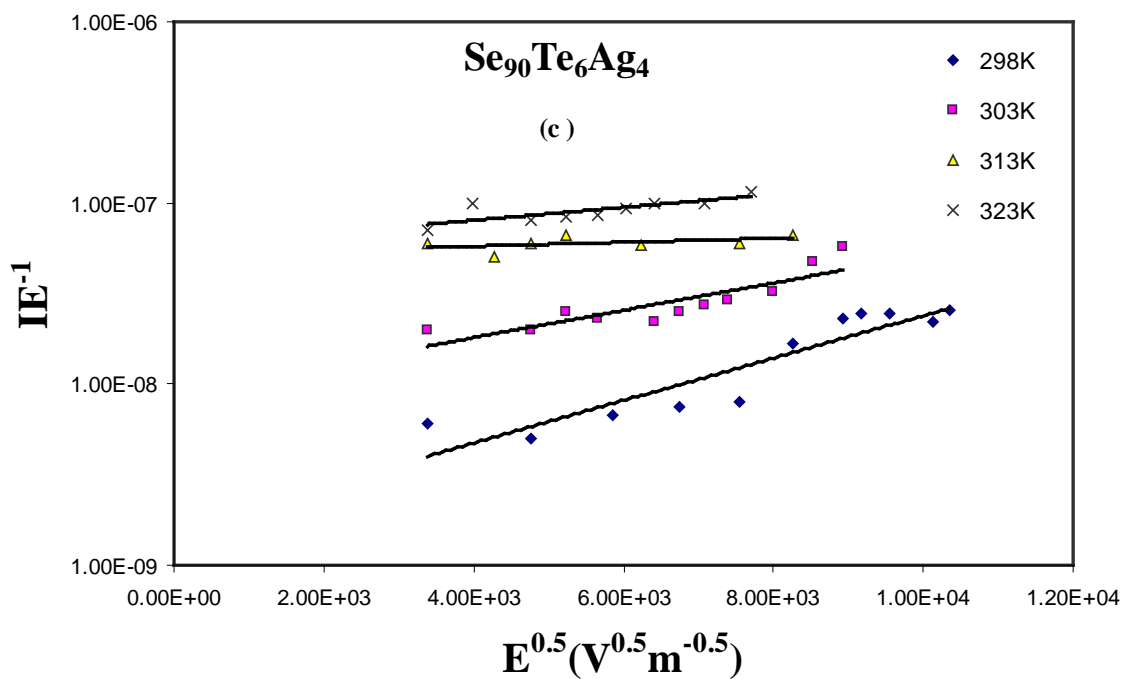


Fig.5(c,d)

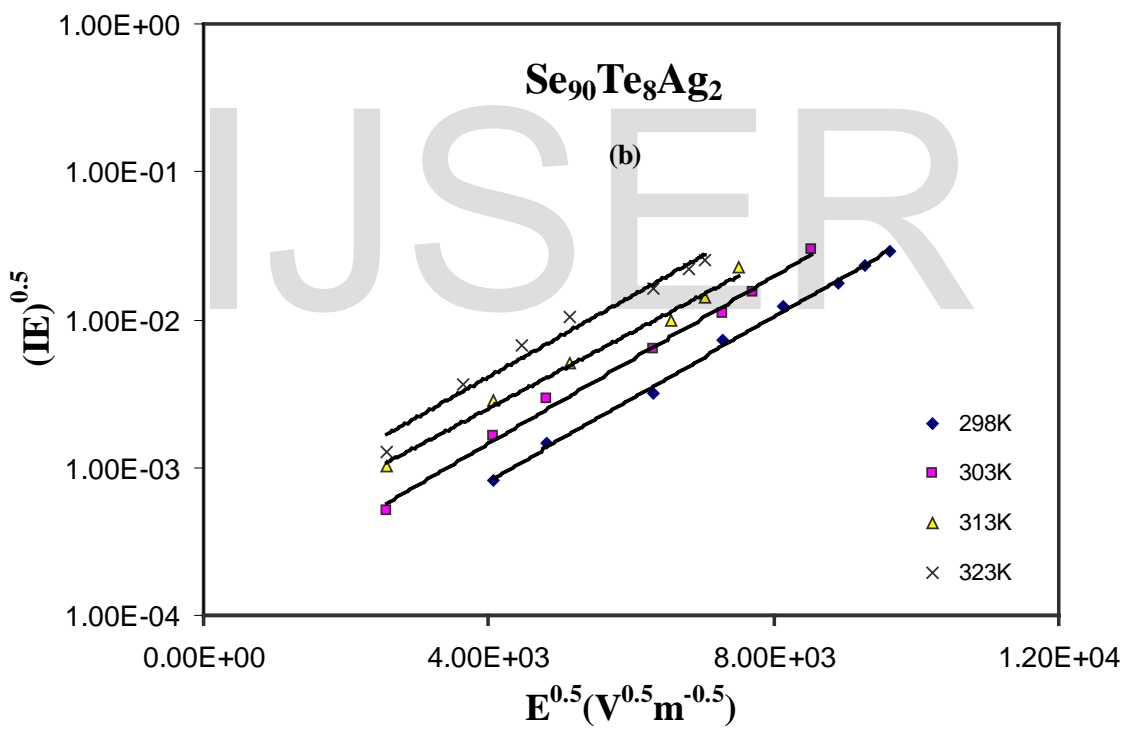
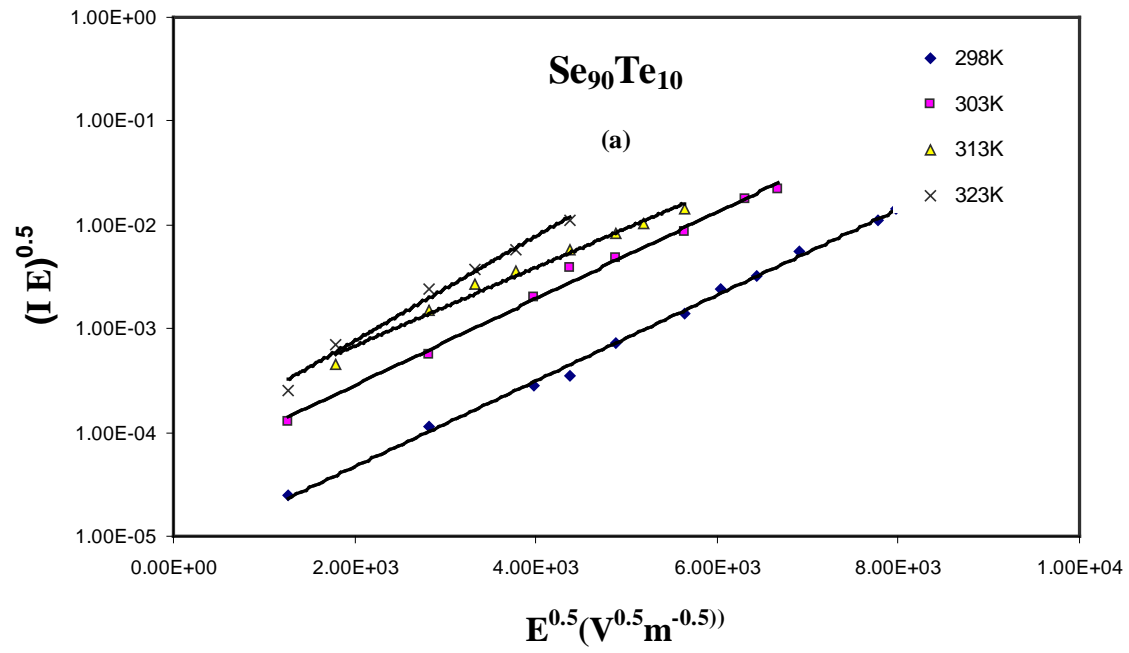


Fig.6(a,b)

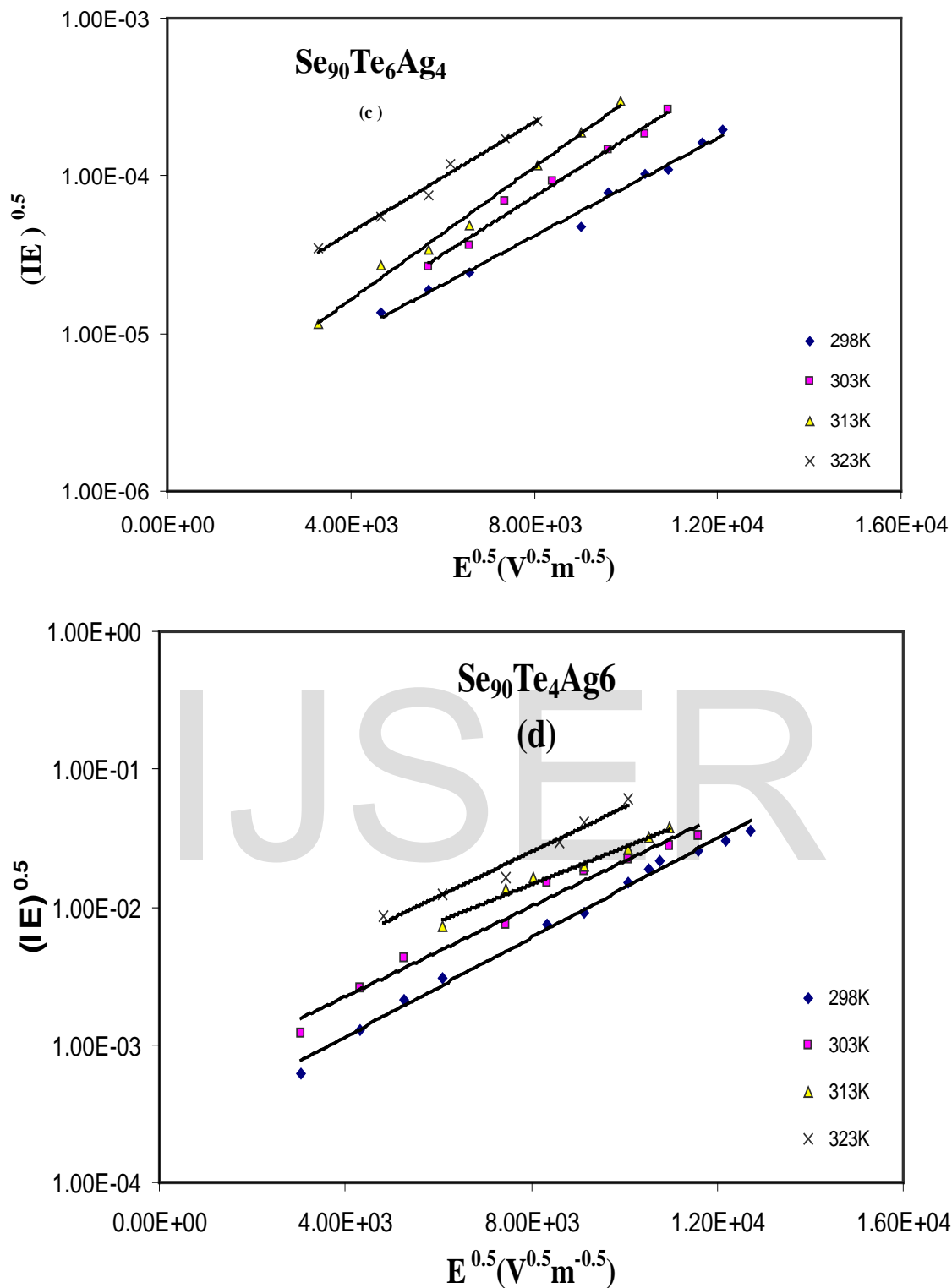


Fig.6(c,d)

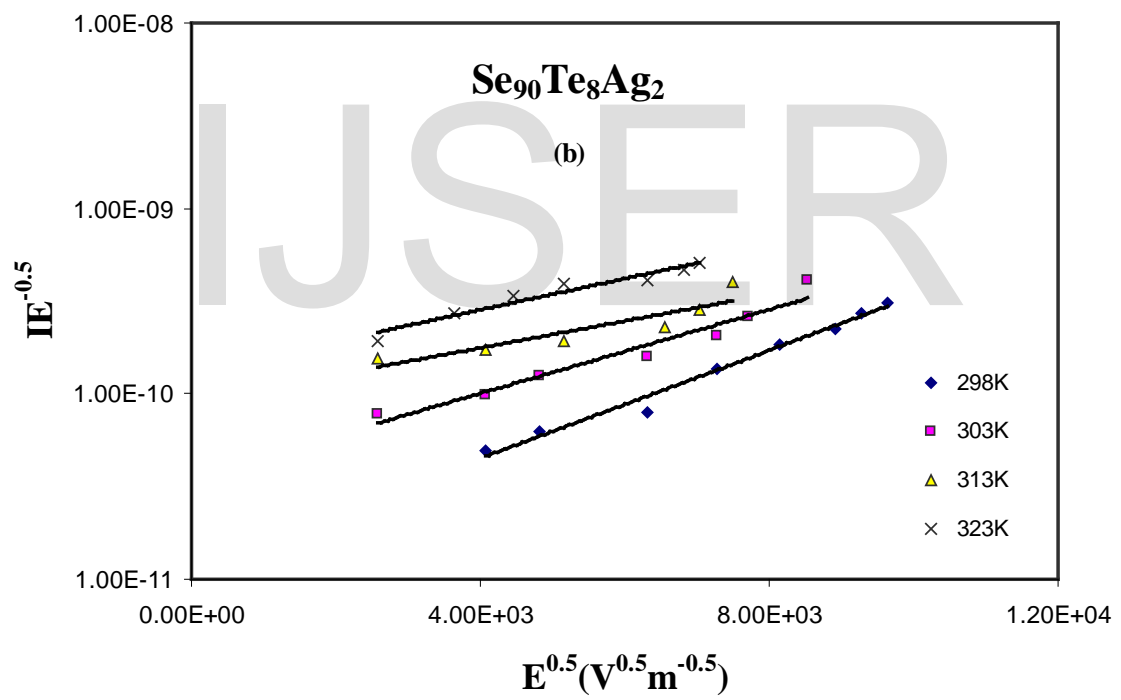
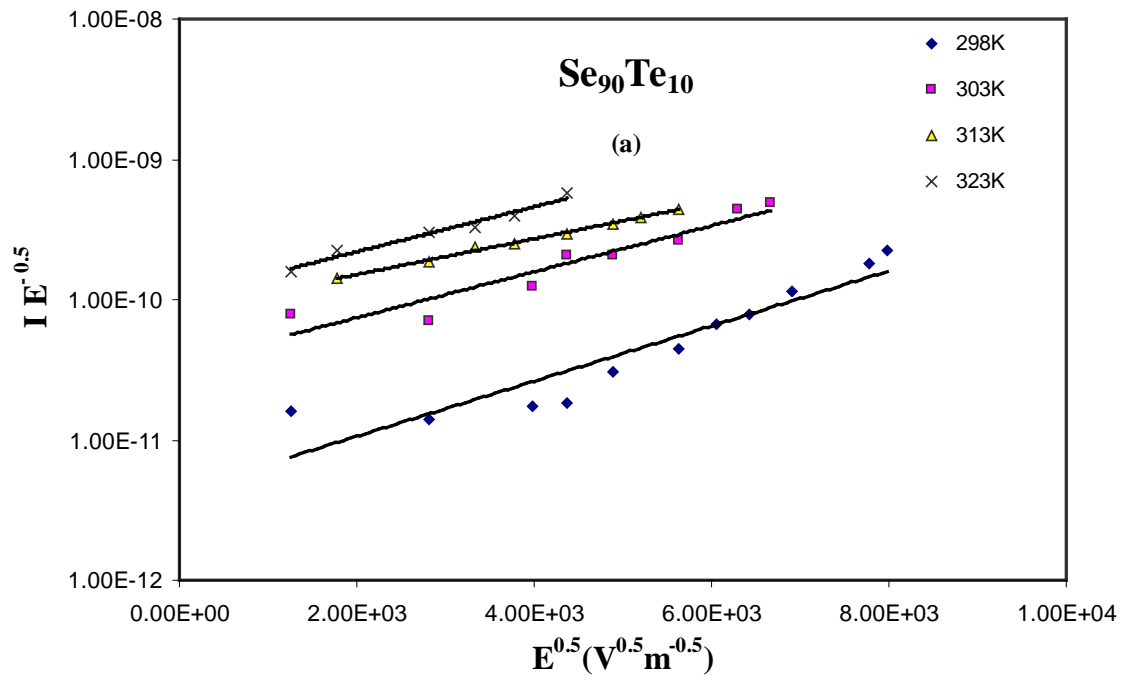


Fig.7(a,b)

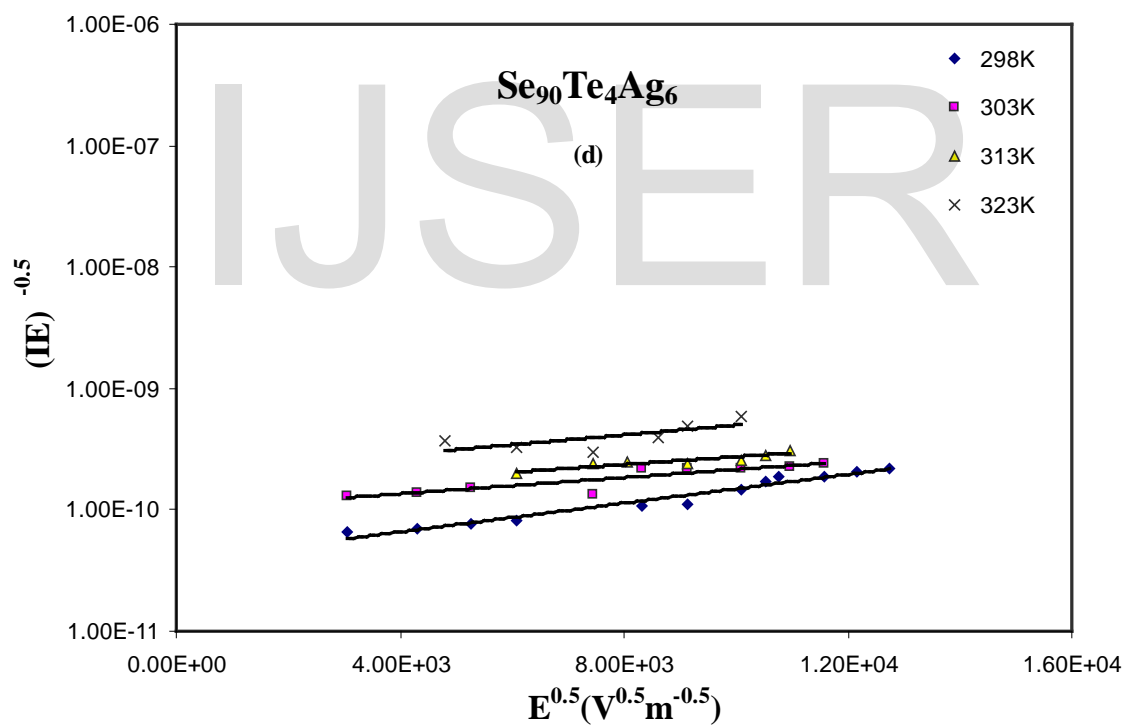
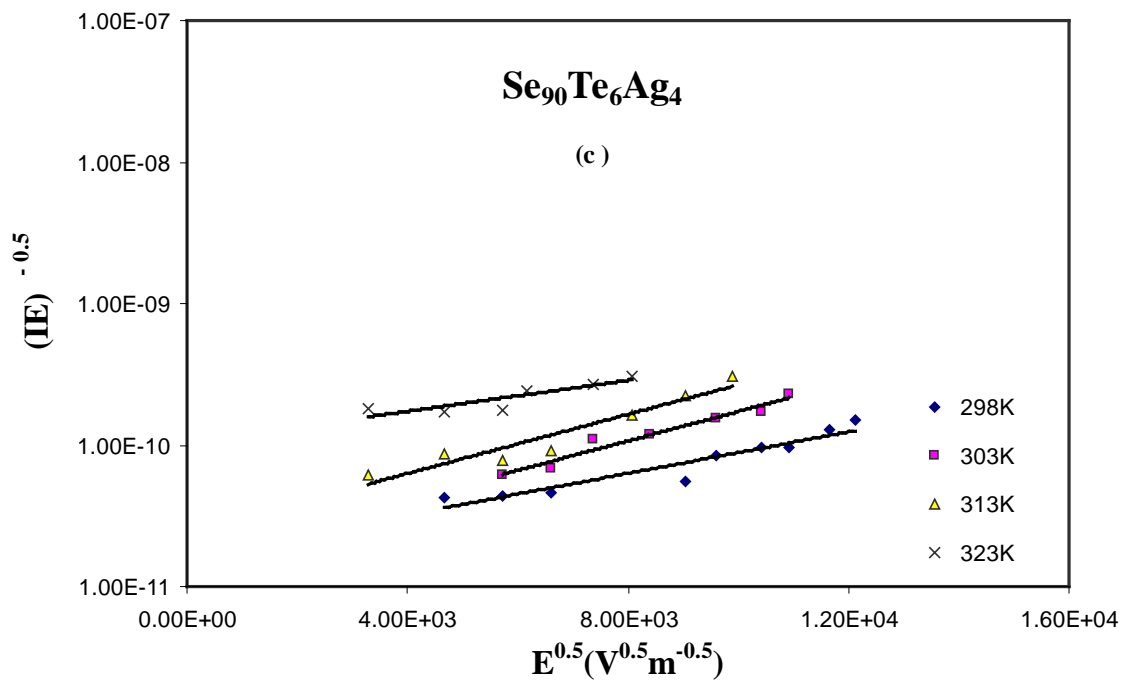


Fig.7(c,d)

Table.(1): Values of dielectric constant, β_{PF} and B_s for $Se_{90}Te_{10-x}Ag_x$ ($x=0,2,4,6$) thin films

Composition	ϵ	$\beta_{PF} \times 10^{-5}, eV m^{1/2} V^{-1/2}$	$\beta_s \times 10^{-5}, eV m^{1/2} V^{-1/2}$
$Se_{90}Te_{10}$	9.058	2.14	1.2606
$Se_{90}Te_8Ag_2$	8052	2.5	1.299
$Se_{90}Te_6Ag_4$	7.53	2.3	1.38
$Se_{90}Te_4Ag_6$	5.08	3.8	1.68

Table.(2): Variation of β , ϵ with temperature for $Se_{90}Te_{10-x}Ag_x$ ($x=0,2,4,6$) thin films according to Pool Frenkel model .

Pool- Frenkel model									
Composition	$Se_{90}Te_{10}$				$Se_{90}Te_8Ag_2$				
	LogI vs $E^{1/2}$		Log IE^{-1} vs $E^{1/2}$		LogI vs $E^{1/2}$		Log IE^{-1} vs $E^{1/2}$		
Temperature	$\beta \times 10^{-5}$ $eV m^{1/2} V^{-1/2}$	ϵ	$\beta \times 10^{-5}$ $eV m^{1/2} V^{-1/2}$	ϵ	$\beta \times 10^{-5}$ $eV m^{1/2} V^{-1/2}$	ϵ	$\beta \times 10^{-5}$ $eV m^{1/2} V^{-1/2}$	ϵ	ϵ
298	3.671	4.272	2.14	12.57	3.67	4.27	2.570	8.717	
303	4.02	3.562	3.267	5.394	3.811	3.962	2.904	6.827	
313	4.449	2.908	3.375	5.054	3.85	3.88	2.999	6.401	
323	5.22	2.113	3.482	4.748	4.17	3.31	3.215	5.570	

Pool- Frenkel model									
Composition	$Se_{90}Te_6Ag_4$				$Se_{90}Te_4Ag_6$				
	LogI vs $E^{1/2}$		Log IE^{-1} vs $E^{1/2}$		LogI vs $E^{1/2}$		Log IE^{-1} vs $E^{1/2}$		
Temperature	$\beta \times 10^{-5}$ $eV m^{1/2} V^{-1/2}$	ϵ	$\beta \times 10^{-5}$ $eV m^{1/2} V^{-1/2}$	ϵ	$\beta \times 10^{-5}$ $eV m^{1/2} V^{-1/2}$	ϵ	$\beta \times 10^{-5}$ $eV m^{1/2} V^{-1/2}$	ϵ	ϵ
298	3.213	5.57	2.337	10.54	3.8	3.987	1.835	17.099	
303	3.92	3.74	2.904	6.827	3.72	4.16	2.221	11.67	
313	3.6	4.44	3.037	6.242	3.671	4.272	2.531	8.987	
323	3.97	3.65	3.214	5.573	3.488	4.732	2.985	6.461	

Table.(3): Activation energy of $Se_{90}Te_{10-x}Ag_x$ ($x=0,2,4,6$) thin films of the same thickness at various applied voltage.

Compositions	Applied voltage		
	1v	2v	3v
$Se_{90}Te_{10}$	0.53	0.53	0.55
$Se_{90}Te_8Ag_2$	0.57	0.61	0.58
$Se_{90}Te_6Ag_4$	0.71	0.71	0.69
$Se_{90}Te_4Ag_6$	0.74	0.77	0.79

Table.(4):Bond energy between elements in the studied system

Bonds	Se-Ag	Te-Ag
Bond energy,kJ/mole	196.56	154.94

Table.(5):Variation of β , ϵ with temperature for $Se_{90}Te_{10-x}Ag_x(x=0,2,4,6)$ thin films according to Joncher model .

Joncher model									
Composition	$Se_{90}Te_{10}$				$Se_{90}Te_8Ag_2$				
	$Log I E^{1/2}$ vs $E^{1/2}$		$Log I E^{-1/2}$ vs $E^{1/2}$		$Log I E^{1/2}$ vs $E^{1/2}$		$Log I E^{-1/2}$ vs $E^{1/2}$		
Temperature	$\beta \times 10^{-5}$ eV m ^{1/2} V ^{-1/2}	ϵ	$B \times 10^{-5}$ eV m ^{1/2} V ^{-1/2}	ϵ	$\beta \times 10^{-5}$ eV m ^{1/2} V ^{-1/2}	ϵ	$\beta \times 10^{-5}$ eV m ^{1/2} V ^{-1/2}	ϵ	
298	5.141	2.17	3.672	4.270	3.427	4.902	3.084	6.053	
303	5.88	1.66	3.733	4.131	3.833	3.918	3.266	5.397	
313	5.062	2.24	4.049	3.511	4.049	3.511	2.892	6.884	
323	5.571	1.86	4.875	2.422	4.64	2.674	3.482	4.748	
Joncher model									
Composition	$Se_{90}Te_6Ag_4$				$Se_{90}Te_4Ag_6$				
	$Log I E^{1/2}$ vs $E^{1/2}$		$Log I E^{-1/2}$ vs $E^{1/2}$		$Log I E^{1/2}$ vs $E^{1/2}$		$Log I E^{-1/2}$ vs $E^{1/2}$		
Temperature	$\beta \times 10^{-5}$ eV m ^{1/2} V ^{-1/2}	ϵ	$B \times 10^{-5}$ eV m ^{1/2} V ^{-1/2}	ϵ	$\beta \times 10^{-5}$ eV m ^{1/2} V ^{-1/2}	ϵ	$\beta \times 10^{-5}$ eV m ^{1/2} V ^{-1/2}	ϵ	
298	2.57	8.717	2.903	6.832	2.056	13.502	1.606	22.323	
303	3.266	5.397	2.613	8.432	2.744	7.644	1.633	21.591	
313	3.6	4.442	3.375	5.054	2.669	8.082	1.755	18.693	
323	3.781	4.027	3.715	4.171	3.715	4.171	2.487	9.308	